PAPER

Check for updates

Reverse Trojan-horse effect decreased wastewater toxicity in the presence of inorganic nanoparticles†

Idoia Martín-de-Lucía, [a] Marina C. Campos-Mañas, [b] Ana Agüera, [b] Ismael Rodea-Palomares, ‡[a] Gerardo Pulido-Reyes, [c] Francisco Leganés,[c] Francisca Fernández-Piñas [c] and Roberto Rosal *[a]

We studied the toxicological interaction of 46 micropollutants from a biologically treated wastewater effluent in mixtures with silica, amine-modified silica, titanium dioxide and magnetite nanoparticles. The pollutants tracked in this work were polar pharmaceuticals belonging to different therapeutic groups, some of their metabolites and artificial sweeteners, the concentrations of which were mostly in the tens to hundreds of ng L^{-1} range. The results showed particularly high adsorption for furosemide, gemfibrozil and the aminopyrine metabolite 4FAA. There was preferential adsorption of the less polar compounds on the less polar nanoparticles. The total amounts of compounds adsorbed and quantified were 13.4, 4.8, 10.8 and 7.1 μg g^{-1} for SiO_2, SiO_2–NH_2, TiO_2 and Fe_3O_4, respectively. The toxicity of wastewater–nanoparticle mixtures was assessed using the bioluminescent cyanobacterium *Anabaena* sp. PCC 7120 CPB4337. The interactions were quantified by means of the combination index (CI)-isobologram method. The binary mixtures of wastewater with SiO_2, SiO_2–NH_2 and TiO_2 displayed antagonism for the lower affected fractions, which corresponded to the lower concentrations. For higher effects and for the Fe_3O_4 nanoparticles over the whole tested range, the mixtures were additive leading to synergism for the higher affected fractions. No internalization was observed. The results showed that the reduced toxicant bioavailability due to the interaction with nanoparticles is relevant for micropollutants at environmental concentrations. The amount of anthropogenic pollutants retained by metal oxide nanoparticles has significant toxicological effects.

Environmental significance

A well-established line of thought considers that the toxicological interactions of chemicals are insignificant at low dose levels, such as those normally found in wastewater or in receiving bodies. However, the presence of nanoparticles, natural or anthropogenic, indicates an important alteration in the environmental fate and toxicity of chemicals. We studied the adsorption of emerging pollutants from a real effluent on four metal oxide nanoparticles and found that the sequestration of pollutants due to adsorption has significant effects on the observed mixture toxicity. We used a non-internalizing photosynthetic organism to show that important antagonism appeared at low effect levels in wastewater–nanoparticle mixtures. To the best of our knowledge, this is the first study reporting the joint toxicity of nanoparticles and complex mixtures of anthropogenic pollutants at environmental concentrations.

Introduction

Wastewater discharges threaten the environmental quality of water bodies. Water pollutants also endanger surface water and groundwater used for drinking purposes and convert the reclaiming of treated wastewater to a controversial issue. Among all chemicals discharged into water bodies, those borne by treated wastewater are of particular concern.[1,2] The chemical status of surface water is difficult to assess and it is usually judged by considering only some selected compounds and their effect on a prescribed set of species.[3] The prediction of anthropogenic chemical stress has been studied in a high number of works, which allowed establishing an additivity paradigm for estimating the toxic effect of chemical mixtures, according to which, chemicals with a common mode of action are described by concentration addition (CA).[4] For chemicals with different modes of action, independent action

[a] *Department of Chemical Engineering, University of Alcalá, E-28871 Alcalá de Henares, Madrid, Spain. E-mail: roberto.rosal@uah.es*
[b] *CIESOL, Joint Centre of the University of Almería-CIEMAT, La Cañada de San Urbano, 04120 Almería, Spain*
[c] *Department of Biology, Faculty of Science, Universidad Autónoma de Madrid, E-28049, Spain*

‡ Current address: Department of Agricultural and Biological Engineering, University of Florida, 284 Frazer Rogers Hall, Gainesville, FL 32611-0570.

This journal is © The Royal Society of Chemistry 2017

Environ. Sci.: Nano, 2017, 4, 1273–1282 | 1273

(IA) is often used.[5–7] Both CA and IA predict the toxicity of a mixture based on the toxicity of individual components.[8,9] The Scientific Committees on Health and Environmental Risks, on Emerging and Newly Identified Health Risks and on Consumer Safety stated that "interactions (including antagonism, potentiation, and synergies) at low exposure levels are either unlikely to occur or toxicologically insignificant".[4] According to this position, the toxicological interactions of chemicals at the levels usually found in wastewater or in receiving bodies would be negligible.

The presence of nanoparticles indicates an important alteration in the environmental fate and toxicity of anthropogenic pollutants as they can significantly affect the partitioning and phase distribution of hazardous organic compounds in water.[10] It has long been recognized that the adsorption of biomolecules modifies the nanoparticle surface. This is the case of proteins in biological environments, the adsorption of which largely governs their biological behaviour.[11] In aqueous environments, the interaction of organic pollutants and nanoparticles has been studied for different types of particles to use them for sequestering contaminants in remediation applications.[12] Surface characteristics have been recognized as an important factor for determining their interaction with toxic pollutants. Jing et al.[13] showed that the modification of nano-SiO$_2$ with cationic surfactants makes them superior sorbents for certain wastewater pollutants due to the hydrophobic effect or hydrogen bonding, depending on the compound. The combined toxicity of nanoparticles and co-contaminants may lead to mixtures displaying synergistic or antagonistic effects depending on the case. Falconer et al. showed that the toxicity of phenanthrene to zebrafish embryos decreased in the presence of multi-walled carbon nanotubes.[14] For the interaction of fullerene soot and malathion, Sanchís et al. reported a vector or Trojan horse effect on the microcrustacean Daphnia magna.[15] To the best of our knowledge, no studies have been reported on the joint toxicity of nanoparticles and complex mixtures of anthropogenic pollutants.

In this work, we studied the toxicological interaction of wastewater micropollutants from a real sample of biologically treated wastewater with nanoparticles of silica, amine-modified silica, titanium dioxide and magnetite. The set was selected in view of their similar nature, their use as engineered nanomaterials and their similarity with natural nanoparticles. As a toxicity endpoint, we have used the bioluminescent response of the cyanobacterium Anabaena sp. PCC 7120 CPB4337. The interactions were assessed using the method of combination index (CI)-isobologram equation.[16]

Experimental section

Materials

High purity analytical standards from Sigma-Aldrich (Steinheim, Germany) were used in this study. All reference standards presented purity higher than 97%. Individual stock standard solutions were prepared at 1000 mg L^{-1} in methanol (MeOH) or acetonitrile (AcN) and stored in amber glass vials at −20 °C. Intermediate solutions (10 mg L^{-1}) were prepared by 10-fold dilution of stock solutions with MeOH. Mixed working solutions containing all analytes were prepared from the intermediate solutions, and were used for spiking samples in the quantifying procedure. AcN and MeOH HPLC grade, formic acid (purity, 98%) and sodium hydroxide (NaOH, >99%) were supplied by Fluka (Buchs, Germany). The biological grade components of culture media were acquired from Conda-Pronadisa (Spain). Ultrapure water was generated from a Direct-Q™ 5 Ultrapure Water Systems (Millipore, Bedford, MA) with a specific resistance of 18.2 MΩ cm.

The nanoparticles used in this study were: (1) SiO$_2$, 99.5% purity, non-porous, 20 nm; (2) amino-modified SiO$_2$, hereinafter SiO$_2$–NH$_2$, 99.8%, 10–20 nm; (3) TiO$_2$, anatase, 6 nm and (4) Fe$_3$O$_4$, 8 nm, the diameters referring to the size of primary particles. Silica nanoparticles were purchased from SkySpring Nanomaterials (Houston, TX) and titanium and iron oxide from PlasmaChem GmbH (Berlin, Germany). The Dynamic Light Scattering (DLS) size and ζ-potential of the nanoparticle suspensions in water and culture medium are listed in Table S1 (ESI†).

Wastewater was collected from the secondary clarifier of a wastewater treatment plant (WWTP) located in Madrid. This plant treats a mixture of domestic and industrial wastewater with a nominal capacity of 13 000 m^3 h^{-1} of raw wastewater. Table S2 (ESI†) lists the main characterization parameters for the wastewater as received. The wastewater was filtered using 0.45 μm PTFE filters and kept frozen (−20 °C) until runs and analyses. All manipulations except the bioassays were performed using dark flasks and avoiding direct exposure to light to avoid photodegradation. All the analytes included in this study have been previously studied by our group and their occurrence in WWTP effluents has been proved and reported in previous studies.[17–19] They comprise a group of 46 organic pollutants, mainly pharmaceuticals belonging to different therapeutic groups, some of their metabolites and artificial sweeteners. The concentrations of pollutants in wastewater, analyzed as indicated below, and the physico-chemical properties of individual compounds are listed in Table S3 (ESI†). No spiking was performed, so the concentrations correspond to the occurrence of micropollutants in the wastewater sample.

Analyses

Wastewater and nanoparticles (100 mg L^{-1}) were put in contact for 24 h at 20 °C under constant stirring in the dark. The experiments were replicated to ensure reproducibility. For the analyses of micropollutants, 20 mL aliquots were filtered using Vivaspin 20 (5 kDa) polyethersulfone ultrafiltration centrifuge tubes. Prior to use, the tubes were carefully washed with ultrapure water and three times with diluted HCl following the manufacturer's prescription. The filter content after contact between wastewater and nanoparticles was washed

1274 | Environ. Sci.: Nano, 2017, 4, 1273–1282

This journal is © The Royal Society of Chemistry 2017

two times with methanol (2 mL + 2 mL). The samples of raw wastewater, filtered water (0.45 μm PTFE) and the two washing liquors were independently analysed for each run performed. Subsequent sample handling was limited to a further filtration step using 0.45 μm PTFE filters and the addition of AcN (AcN:H$_2$O 10:90, v/v, with surrogates caffeine C13 and cyclophosphamide d4 at 0.5 μg L^{-1} to provide a control injection). All the analyses were duplicated for each sample, including replicates. During contact experiments, samples were kept in the dark to avoid photochemical reactions and the production of oxidation intermediates from wastewater micropollutants. Before analyses, the samples were stored at −20 °C in glass bottles.

The detection and quantification of the microcontaminants was performed by liquid chromatography coupled to hybrid quadrupole/linear ion trap mass spectrometry (LC-QqLIT-MS/MS) using an Agilent 1200 LC system (Agilent Technologies, USA) and a 5500 QTRAP LC/MS/MS from AB Sciex Instruments (USA). Chromatographic separation was performed using a ZORBAX Eclipse XDB C18 analytical column of 50 mm × 4.6 mm I.D (1.8 μm particle size) from Agilent. Two methods were used with mobile phases A and B being MilliQ water (containing 0.1% formic acid) and AcN, respectively. In method 1, the gradient program was set as follows: 10% B (initial conditions, 1 min), then increased to 50% within 4 min, further increased to 100% within 10 min, kept constant 4 min and reduced to 10% in 0.1 min. The total run time was 14.1 min and the post-run equilibrium time was 4 min. In method 2, the percentage of B changed linearly as follows: 0 min, 10%; 6 min, 100%; 9 min, 100%; 9.1 min, 10%; 12 min, 10% with a total run time of 12 min. The sample injection volume was 10 μL and the flow rate was kept constant at 0.4 mL min^{-1} in both methods.

The LC system was connected to the MS by a TurboIon Spray source operated in positive and negative ionization modes. Source settings were: IonSpray voltage (IS), 4500 V in positive and −4500 V in negative mode; source temperature, 550 °C; CAD gas, medium; ion source gas 1, 50 psi; for both methods. Ion source gas 2, 40 psi for method 1 and 50 psi for method 2 and curtain gas, 25 for method 1 and 20 for method 2 (arbitrary units). Nitrogen was used as the nebulizer gas, curtain gas and collision gas.

Analyses were performed in selected reaction monitoring (SRM) mode with Scheduled MRM™ algorithm and 60 s window time. Analytes were confirmed by two SMR transitions at the right retention time and with the correct SMR ratio in accordance with the EU guidelines for LC-MS/MS analysis (Decision 2002/657/EC). Data were acquired using Analyst Software 1.5.1 and processed with MultiQuant 3.0.1 software (Applied Biosystems).

High-resolution transmission electron microscopy (TEM) images were obtained using a JEOL JEM 1400 microscope operating at 100 kV in combination with energy dispersive X-ray spectroscopy (EDS). The TEM sample preparation is described in detail in the ESI.† The staining of lipid droplets was performed using boron dipyrromethene difluoride

(Bodipy) 505/515. The process is also described in the ESI.† ICP-MS analyses of metals released were performed using an ICP-MS model X Series 2 system apparatus from Thermo Scientific.

Toxicity bioassays

Anabaena sp. PCC 7120 strain CPB4337 was used in this study as a bioreporter of nanoparticles and wastewater toxicity. This strain bears in the chromosome a Tn5 derivative with *lux*CDABE from the luminescent terrestrial bacterium *Photorhabdus luminescens*. The toxicity bioassays using the recombinant bioluminescent cyanobacterium *Anabaena* CPB4337 are based on the inhibition of constitutive luminescence caused by the presence of toxicants.[20] *Anabaena* CPB4337 was routinely grown at 28 °C under light (*ca.* 60 μmol photons m^2 s^{-1}) on a rotatory shaker at 135 rpm in 100 mL AA/8 (ref. 21) supplemented with nitrate (5 mM) (hereinafter AA/8+N).

The assays were conducted in transparent sterile 24-well microtiter plates in a total volume of 1.5 mL. Cyanobacterial cultures, grown as described, were maintained in batch cultures for 72 h starting with OD$_{750nm}$ = 0.2 until a final OD$_{750nm}$ = 0.6–0.8 measured using a Hitachi U-2000 spectrophotometer. *Anabaena* CPB4337 cells, prepared as described, were added to the wells together with the required amount of nanoparticles from concentrated stock solutions to get the desired final exposure concentrations. The nanoparticle concentrations tested ranged from 1 to 500 mg L^{-1} for SiO$_2$ and SiO$_2$–NH$_2$, 0.1–100 mg L^{-1} for TiO$_2$ and 1–100 mg L^{-1} for Fe$_3$O$_4$. In all cases, stock nanoparticle suspensions were freshly prepared in AA/8+N a few minutes prior to toxicity assays to ensure the homogeneity of the stock suspensions and to prevent undesired ageing or aggregation. The suspension was dispersed using a Sonics VibraCell ultrasound disperser (BioBlock Scientific, France) operating at 500 W. Wastewater was serially diluted with tenfold concentrated AA/8+N so that cultures were exposed to a dilution in the 0.125–1 range. The 24-well microtiter plates were kept at 28 °C under continuous illumination, *ca.* 40 μmol photons m^{-2} s^{-1} on a rotatory shaker for 24 h. Samples were taken after 1 h, 4 h, and 24 h and transferred to white 96-well microtiter plates for luminescence measurements in a Centro LB 960 luminometer. Three independent experiments with quadruplicate controls were performed for each nanoparticle concentration or wastewater dilution.

EC$_{50}$ values, the median effective concentration of nanoparticles or wastewater dilution that causes 50% inhibition of constitutive luminescence with respect to a non-treated control and their related statistical parameters were estimated using a linear interpolation method and computed using the software ICp, available from the Environmental Protection Agency.[22] The ICp approach uses a nonparametric monotonic regression that does not depend on any particular model allowing point estimates and confidence intervals even without the entire dose–response curve.[23]

This journal is © The Royal Society of Chemistry 2017

Environ. Sci.: Nano, 2017, **4**, 1273–1282 | 1275

To evaluate the nature of the interaction of nanoparticles with wastewater, binary combinations of each nanoparticle and wastewater were prepared and tested using serial dilutions with a fixed ratio based on their individual EC_{50} values. Five dilutions (serial dilution factor of 1.5) of each nanoparticle and wastewater and their combinations were tested in independent experiments with quadruplicate samples as described elsewhere.[16,24] Additional details are provided in the ESI.† The data were analysed using the computer program CompuSyn to determine the dose-effect curve parameters and combination index (CI) values of the different mixtures in the whole range of effect levels.[25] CI < 1, CI = 1 and CI > 1 indicate synergism, an additive effect and antagonism, respectively.

Results and discussion

The micropollutants adsorbed on the nanoparticle surface were quantified by comparing the 5 kDa filtrate after wastewater contact with blank runs, which were the same wastewater samples manipulated and filtered under the same conditions but in the absence of nanoparticles. Fig. 1 shows the amount of compounds adsorbed for which the concentration difference with respect to the blanks was significant at the 95% confidence level. The total amount of compounds significantly adsorbed was 13.4 µg g^{-1}, 4.8 µg g^{-1}, 10.8 µg g^{-1} and 7.1 µg g^{-1} for SiO_2, SiO_2–NH_2, TiO_2 and Fe_3O_4, respectively. The analytical results showed that the higher amounts adsorbed corresponded to 4AAA, 4FAA, furosemide, gemfibrozil, iopamidol, ranitidine and trimethoprim for SiO_2; 4AA, 4FAA, bezafibrate, furosemide, gemfibrozil and hydrochlorothiazide for SiO_2–NH_2; 4AAA, 4FAA, furosemide, gemfibrozil, iopamidol and trimethoprim for TiO_2 and 4AAA, 4FAA, bezafibrate, furosemide, gemfibrozil, propranolol and sulfa-

methoxazole for Fe_3O_4. Relative to their occurrence in wastewater, the compounds retained at >40% were: gemfibrozil (43%), propranolol (54%) and trimethoprim (40%) for SiO_2; propranolol (49%) for SiO_2–NH_2; gemfibrozil (40%), propranolol (54%) and trimethoprim (43%) for TiO_2 and propranolol (50%) for Fe_3O_4.

Fig. S1 (ESI†) illustrates the adsorption of individual compounds as bubbles proportional to the amount adsorbed and as a function of K_{ow}, and D_{ow}, which are the octanol–water and the pH-dependent (or apparent) octanol–water distribution coefficients, respectively. The difference between K_{ow} and D_{ow} is that D_{ow} considers the dissociation constant of acidic or basic solutes using the Henderson–Hasselbalch equations (the derivation of D_{ow} is explained in detail in the ESI†). D_{ow} represents the tendency of a given chemical to partition between an organic phase and an aqueous phase at a given pH, which is 7.8 in our case. Chemicals with low D_{ow} values are considered hydrophilic, while higher values correspond to compounds with lower water solubility and higher soil or sediment adsorption coefficients. Fig. 2 shows the cumulative amount of compounds significantly adsorbed onto the four nanomaterials as a function of their log D_{ow} value in growing order of D_{ow}. Although the chemicals studied in this work were all hydrophilic, there was a clear difference in the adsorption capacity of metal oxides, particularly SiO_2 and TiO_2, with considerably higher adsorption capacity for the less polar and less hydrophilic compounds. The higher amounts adsorbed corresponded to SiO_2 and to the hydrophobic TiO_2. The surface-charged derivative SiO_2–NH_2 and Fe_3O_4 retained a considerably lower amount of micropollutants.

It is interesting to note that the compounds adsorbed on the nanoparticles could not be completely removed after two consecutive washings with methanol, meaning that the
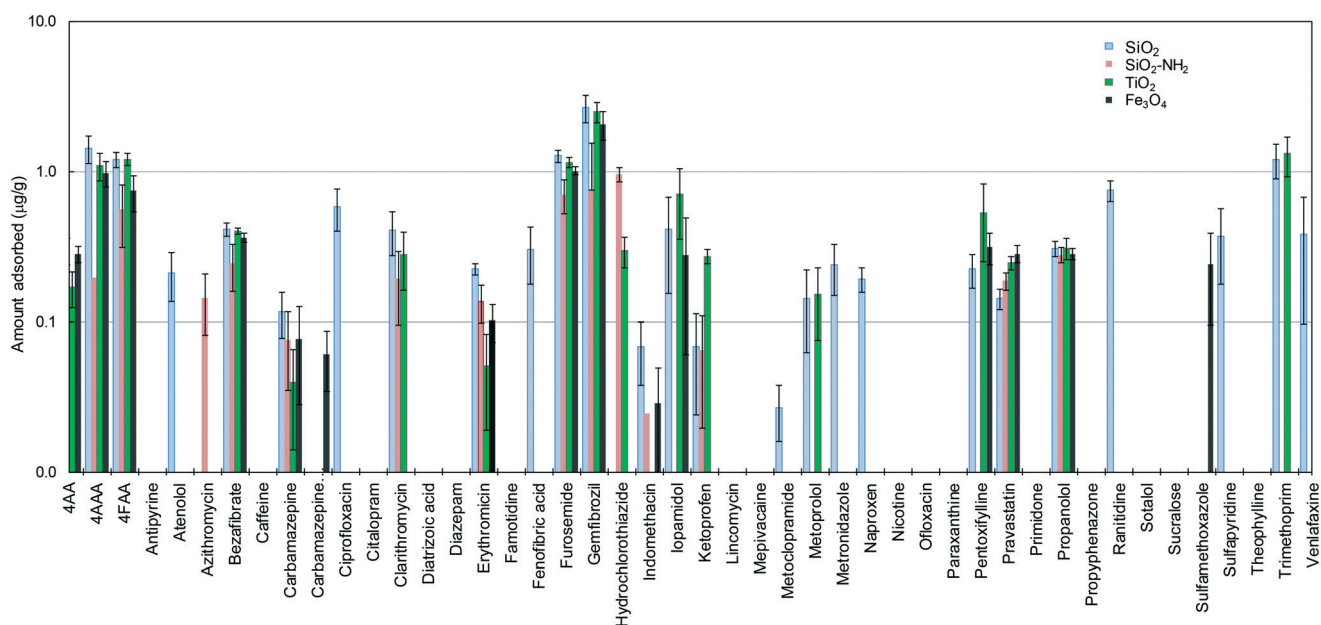

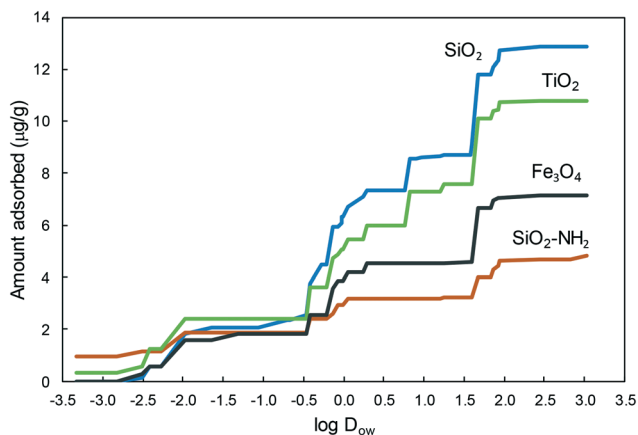Fig. 1 Amount of pollutants adsorbed on different nanoparticles after 24 h in contact with wastewater.

1276 | Environ. Sci.: Nano, 2017, 4, 1273–1282

This journal is © The Royal Society of Chemistry 2017

Fig. 2 Amount of pollutants adsorbed on the different nanoparticles as a function of their apparent octanol–water partition coefficient, log D_{ow}.

adsorption was relatively strong. In most cases, the percentage of the compound recovered after methanol washing was in the 70–90% range, and, therefore, 10–30% of the compound still remained adsorbed after the double extraction. Notably, for propranolol and clarithromycin the amount recovered was only ~50% (Fig. S2, ESI†). The interaction of adsorbates and colloids has been the subject topic of many studies and theoretical approaches.[26] The surface of oxides consists of an array of cationic acid centres and anionic oxygen centres acting as a Lewis base. Surface hydroxyl groups can act as Brønsted acid or base sites and form hydrogen bonds with electronegative atoms. Besides, the surface of oxides becomes hydrated in aqueous medium favouring the interaction of polar organics through hydrogen bonding or polar interactions.[27] Consequently, metal oxides exhibit hydrophilic surfaces, which interact preferentially with compounds in the 0–2 log D_{ow} range, which are still hydrophilic but less prone to remain in the aqueous phase than those with lower D_{ow}.

The results indicated that the charge of the organic compounds did not influence the extent of their adsorption. For example, gemfibrozil is a fibric acid derivative with pK_a 4.5, and was completely dissociated at the pH of wastewater, while propranolol is a basic compound (pK_a 9.4) with a positively charged amino moiety at pH 7.8 (the pH of all the experiments). However, the amounts of these two compounds adsorbed on the different nanomaterials were not particularly different (Fig. 1). The reason was that the difference in the intrinsic charge (measured as ζ-potential) of the nanoparticles, which ranged from −26.5 mV (SiO$_2$) to +42.6 mV (Fe$_3$O$_4$) in water, disappeared when dispersed in wastewater in which the ζ-potential was essentially coincident with that of wastewater particles due to heteroaggregation with natural colloids. In AA/8+N medium, the particle charge was also essentially coincident with that of the background medium except for SiO$_2$–NH$_2$ at high concentration due to the influence of its positively charged amines (Table S1†). Our results showed that most of the differences found among the nanoparticle suspensions in pure water could not be observed in

wastewater. The heteroaggregation of nanoparticles with natural colloids and the adsorption of natural organic matter explain the results obtained.[28] Accordingly, the suspensions of nanoparticles in wastewater led to colloids with a size distribution in the hundreds of nanometre range. In pure water, however, some minor peaks in the tens of nanometre range were also detected, which corresponded to lower range aggregates, probably in a dynamic equilibrium with the larger ones. The influence of particle agglomerates in the adsorption capacity of nanosized materials has been frequently studied and the findings reflect that the adsorption parameters did not vary greatly despite the large differences in nanoparticle aggregation/agglomeration.[29] As shown by DLS and the micrographs below, the nanoparticles tend to form clusters, which are generally loose nanoparticle agglomerates. This fact suggests that the sites on the primary particles remain accessible for solutes, and the adsorption kinetics, rather than the equilibrium concentration, could be affected by particle agglomeration. The contact time (24 h) was chosen on this basis.

The toxicity of the studied nanoparticles and wastewater to *Anabaena* CPB4337 in 1, 4 and 24 h assays are listed in Table 1 as EC$_{10}$, EC$_{20}$ and EC$_{50}$ (in case a bioluminescence inhibition >50% was attained). SiO$_2$ nanoparticles were nontoxic, with EC$_{50}$ (24 h) near the maximum concentration tested in this work (500 mg L^{-1}). The same holds for SiO$_2$–NH$_2$ for which a 24 h luminescence inhibition over 50% was only attained at 443 (±18) mg L^{-1}. For a lower exposure time, EC$_{50}$ was not reached, but EC$_{10}$ and EC$_{20}$ could be successfully recorded and could be used as surrogates for the classic hypothesis-based no effect concentration, NOEC.[30] It is noteworthy that TiO$_2$ and Fe$_3$O$_4$ nanoparticles, which were more toxic in terms of EC$_{50}$, displayed EC$_{10}$ values higher than those of SiO$_2$ and SiO$_2$–NH$_2$ for 4 and 24 h (and very similar after 1 h) in contact with *Anabaena* cells. The EC$_{10}$ values, which are below 1 mg L^{-1} for SiO$_2$ and SiO$_2$–NH$_2$, revealed remarkably low NOEC values for these particles.

Wastewater toxicity is given as the dilution factor, 1 corresponding to undiluted wastewater for which 51.1% inhibition (48.9–53.3) was recorded. The maximum dilution tested was 0.125 (12.5% wastewater in 87.5% pure water), which yielded 15.3% luminescence inhibition (13.7–16.8). The slight toxicity recorded as EC$_{10}$ for wastewater during 1 h tests was not observed for longer exposures, probably because of the stimulation associated with nutrients in wastewater.[31] No evidence of particle settling was observed at the bottom of the wells during the exposure period. The presence of free ions was considered for titanium, because iron is an essential metal and silicon cannot exist free in solution. The results showed that for TiO$_2$ concentrations up to 500 mg L^{-1}, the concentration of the titanium ion was below the detection limit when analysed by ICP-MS in 5 kDa ultrafiltrates after 24 h in contact with the growth medium. The concentration–response curve for 24 h luminescence inhibition is shown in Fig. 3 for wastewater and nanoparticles over the entire concentration range studied.

This journal is © The Royal Society of Chemistry 2017

Environ. Sci.: Nano, 2017, **4**, 1273–1282 | **1277**

Table 1 Dose-effect parameters for the luminescence inhibition of *Anabaena* CPB4337 in 1, 4 and 24 h assays

Hours	EC_x value	Wastewater[a]	SiO_2	$SiO_2–NH_2$	TiO_2	Fe_3O_4
1	EC_{10}	0.15 ± 0.01	3.6 ± 1.3	1.9 ± 1.4	3.7 ± 0.5	3.9 ± 1.4
	EC_{20}	0.41 ± 0.01	25.4 ± 3.0	23.9 ± 2.9	8.3 ± 2.2	9.3 ± 2
	EC_{50}	—	—	—	57 ± 20	29 ± 2
4	EC_{10}	—	0.65 ± 0.04	0.72 ± 0.04	2.3 ± 1.0	4.9 ± 2
	EC_{20}	0.20 ± 0.01	18.3 ± 1.8	16.8 ± 1.7	5.0 ± 1.1	10 ± 3
	EC_{50}	0.69 ± 0.03	—	—	15 ± 1	28 ± 2
24	EC_{10}	—	0.56 ± 0.02	0.62 ± 0.04	0.92 ± 0.67	8.2 ± 2
	EC_{20}	0.33 ± 0.02	6.8 ± 2.3	8.5 ± 1.2	2.9 ± 1.4	15 ± 2
	EC_{50}	0.94 ± 0.02	451 ± 16	443 ± 18	14 ± 2	33 ± 2

[a] Wastewater dilution (1 = undiluted).

The data available on the toxicity of the tested nanoparticles to cyanobacteria are limited to *Anabaena variabilis*, for which the inhibition of growth rate and nitrogen fixation activity after 96 h exposure to 10 nm TiO_2 nanoparticles was reported as (EC_{50}) 0.62 mg L^{-1} and 0.4 mg L^{-1}, respectively.[32] The exposure of *Anabaena variabilis* to TiO_2 nanoparticles led to ROS production, membrane damage, the opening of intra-thylakoidal spaces and internal plasma membrane disruption, clearly due to the photocatalytic activity of TiO_2, and without evidence of internalization. In the absence of other data, the results can be compared with those for green algae. The growth inhibition of *Scenedesmus obliquus* exposed to 10–20 nm SiO_2 nanoparticles yielded EC_{20} values for 72 and 96 h assays of 388.1 mg L^{-1} and 216.5 mg L^{-1}, respectively.[33] Lower values were reported for the 72 h growth inhibition of the alga *Pseudokirchneriela subcapitata* exposed to 12.5 and 27.0 nm SiO_2 nanoparticles (EC_{20} of 20.0 ± 5.0 mg L^{-1} and 28.8 ± 3.2 mg L^{-1}, respectively).[34] Many results have been published concerning the toxicity of TiO_2 nanoparticles particularly to the green alga *Pseudokirchnieriella subcapitata* and for 72 h standard tests, although they are often difficult to compare due to the photocatalytic activity of TiO_2 nano-

particles. The EC_{50} for P25 Evonik-Degussa TiO_2 (21 nm) was 2.53 mg L^{-1}.[35] The EC_{20} and EC_{50} for 25–70 nm TiO_2 were 1.81 mg L^{-1} and 5.83 mg L^{-1}, respectively.[36] The toxicity of TiO_2 to *Desmodesmus Subspicatus* increased with decreasing particle size with EC_{50} as low as 44 mg L^{-1} for 25 nm particles.[37] The toxicity of Fe_3O_4 to *Pseudokirchneriella subcapitata* was 1.93 ± 0.69 mg L^{-1}.[38] The results obtained in this work were coincident with most literature data, TiO_2 and Fe_3O_4 being relatively toxic for the cyanobacterium with EC_{50} at the tens of mg L^{-1} levels.

The fitting parameters for the nanoparticle–wastewater combinations are given in Table S4† (obtained using the software CompuSyn). Fig. 4 shows the combination index plot for binary nanoparticle–wastewater combinations within the experimental range of affected fractions assayed in this work. The graphs were plotted by interval averaging the values from five different assays and the combination index (CI) < 1, CI = 1 and CI > 1 indicate synergism, an additive effect and antagonism, respectively. Fig. 4a shows SiO_2 and $SiO_2–NH_2$ mixtures with wastewater while Fig. 4b displays the results of TiO_2 and Fe_3O_4–wastewater mixtures after 24 h exposure. Fe_3O_4 mixtures with wastewater were additive all throughout the experimental range of bioluminescence inhibition (f_a). The other three nanoparticles, SiO_2, $SiO_2–NH_2$ and TiO_2 behaved in a similar way and displayed antagonism for the lower affected fractions, which corresponded to the lower concentrations of constant-ratio mixtures. For increased bioluminescence inhibition, a plateau was observed in the antagonism-additivity range of affected fractions, which can be roughly defined as 0.5 < CI < 2.[39,40] Higher affected fractions, corresponding to the higher dosages of wastewater and nanoparticles, displayed a slight tendency towards synergism. The antagonism corresponded in all cases to the lower exposure concentrations. As the concentration increased, the behaviour approached additivity, which is the opposite trend expected for conventional mixtures of chemicals, in which interactions usually are supposed to occur at medium or high dose levels, being unlikely or insignificant for the lower effects.[4]

Nanoparticles are not classic chemical toxicants. They form aggregates/agglomerates in water or aqueous culture media that can entrap cells. This mechanism has been proposed before to explain algal growth inhibition.[23]
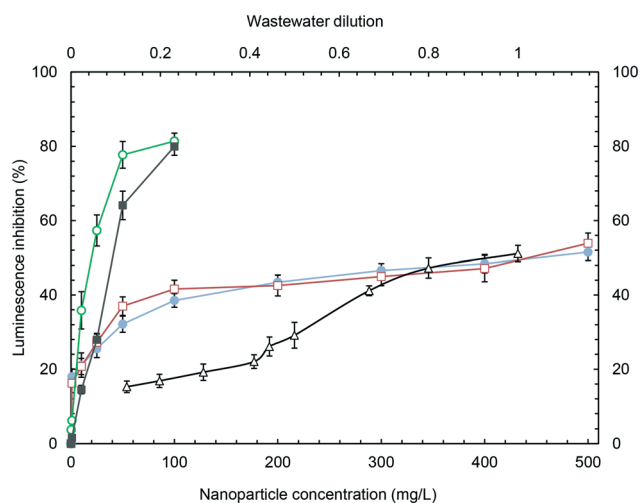

Fig. 3 Toxicity of different nanoparticles to *Anabaena* CPB4337 test: SiO_2 (●), $SiO_2–NH_2$ (□), TiO_2 (○), and Fe_3O_4 (■). Upper scale and open triangles (△): wastewater toxicity (1: non-diluted samples). Exposure time: 24 h.
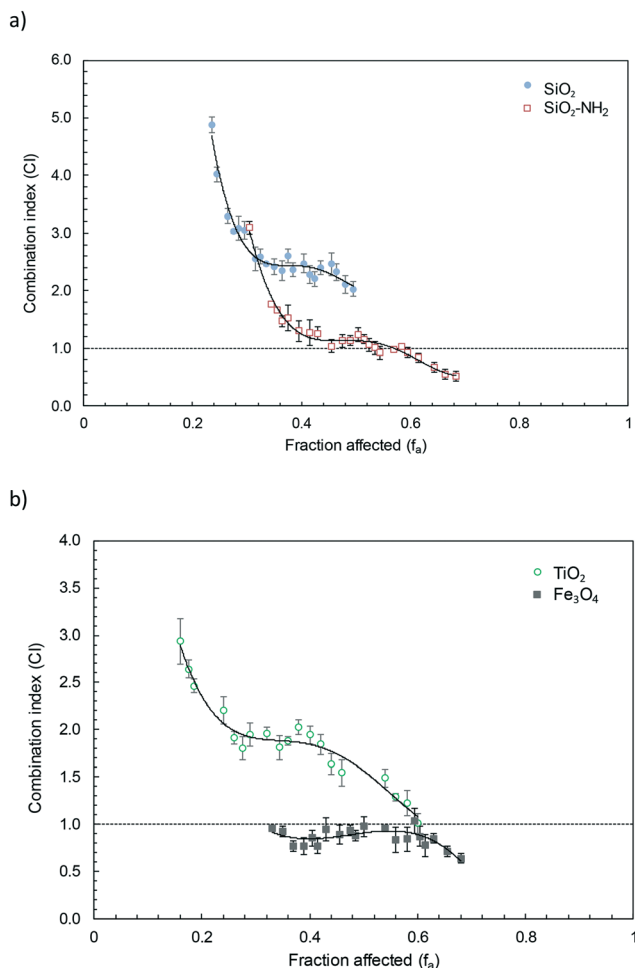
a)

b)

Fig. 4 Combination index plot for binary nanoparticle–wastewater combinations. 4a: SiO$_2$–wastewater (●), SiO$_2$–NH$_2$–wastewater (□). 4b: TiO$_2$–wastewater (○), Fe$_3$O$_4$–wastewater (■). CI values are plotted as a function of the fractional inhibition of bioluminescence (f_a) within the experimental range. CI > 1 indicates antagonism and the dotted line additivity. Exposure time: 24 h.

Heteroaggregation, driven by natural organic matter (NOM) or exopolymeric exudates, is also known to influence the concentration–response relationship of nanoparticles.[41] Several studies revealed different kinds of pollutant–nanoparticle interactions of toxicological relevance. The presence of TiO$_2$, bare and polyacrylate coated, reduced the toxicity of cadmium ions due to their sorption/complexation, which would reduce bioavailability.[42,43] The effect of NOM is a well-known factor influencing nanotoxicity. The EC$_{50}$ value reported for the growth inhibition of *P. subcapitata* exposed to TiO$_2$ nanoparticles was 0.27 mg L^{-1}, but no growth inhibition was observed in a medium containing 8 mg L^{-1} NOM.[44] The effect of NOM has been associated with lower colloidal stability and higher particle aggregation, which largely depends on surface characteristics.[45]

We found high adsorption of some wastewater pollutants toxic to cyanobacteria and algae. Gemfibrozil, which was strongly adsorbed (Fig. S2†), was toxic to the cyanobacterium *Anabaena* with 24 h EC$_{50}$ of 4.4 mg L^{-1}.[46] Table S5† lists the

literature data for most of the wastewater pollutants identified in this work. Other toxic compounds adsorbed on the nanoparticle studied in this work are clarithromycin, sulfamethoxazole, propranolol and trimethoprim. It is difficult to make quantitative predictions on the toxicity reduction that could be attributed to compounds sequestered by nanoparticles. First, it is due to the scarcity of toxicity data available for cyanobacteria, but also due to the presence of many other micropollutants in real wastewater. The changes in the bioavailability of contaminants due to the vector function of nanoparticles has been demonstrated for carbon nanomaterials.[15] The interaction of nanosized oxides with wastewater pollutants is weak with non-polar compounds due to the strong competition with water molecules for hydrophilic surface sites.[47] However, polar compounds are known to interact with considerable strength with oxides.[48] In real environments, the surface modification with NOM was also shown to enhance the sorption of organic compounds.[49] We showed that significant and relatively strong adsorption of relevant micropollutants takes place in the presence of nanoparticles, the combination resulting in an antagonistic toxic effect. The antagonism decreased for higher exposure levels, turning into additive or synergistic behaviour, as expected if the nanoparticle surface becomes saturated with organic compounds. The occurrence of synergistic interactions in pollutant–wastewater mixtures was previously observed for the higher range of concentrations.[50] It has been stated that the experiments showing significant synergy refer to fairly high concentrations with limited environmental relevance.[51] However, experimental evidence of non-additive interactions using environmental concentrations of organic micropollutants has not been previously reported. As for the nanoparticles, the models predict environmental concentrations in the 1–100 µg L^{-1} range. However, typical colloidal matter can be found at 1–10 mg L^{-1} in surface waters. It is noteworthy that the similitude of the nanoparticles tested in this work with natural inorganic colloids, mainly constituted of silicates, and metal oxides and hydroxides in the submicron size and in stable suspension in water.[52] For the case of Fe$_3$O$_4$–wastewater mixtures, no antagonism was observed at low affected fractions. The probable reason is that the toxicity reduction associated with the adsorption of pollutants was lower due to the lower adsorption of basic compounds on positively charged surfaces (the ζ-potential recorded for Fe$_3$O$_4$ in water was +32.4 ± 0.3 mV at 10 mg L^{-1}, as indicated in Table S1†). This would explain the low adsorption of the antibiotics trimethoprim and clarithromycin with respect to TiO$_2$ or azithromycin and hydrochlorothiazide with respect to SiO$_2$–NH$_2$.

The localization of nanoparticles and the ultrastructural changes induced in *Anabaena* CPB4337 by nanoparticles, wastewater and nanoparticle–wastewater mixtures after 24 h of exposure are shown in Fig. 5. Non-exposed cells kept their cell envelopes intact (Fig. 5a). The cyanobacterial cells exposed to SiO$_2$ and SiO$_2$–NH$_2$ nanoparticles did not show any remarkable changes in their ultrastructure (Fig. 5c and d).

This journal is © The Royal Society of Chemistry 2017

Environ. Sci.: Nano, 2017, **4**, 1273–1282 | 1279

Fig. 5c clearly shows large aggregates of SiO_2 nanoparticles gathering away from the cells. This effect cannot be attributed to the presence of EPS (exopolymeric substances) as this strain does not produce them. EDS analysis assigned silicon as the main constituent of nanoparticle aggregates. In agreement with our results, other authors did not observe significant changes in shape and cell morphology in the green alga *P. subcapitata* exposed to SiO_2 nanoparticles. We did not find any evidence of particle uptake.[34] As shown in Fig. 5e, TiO_2 nanoparticles were observed surrounding and adhering to the outer surface of cyanobacterial cells. The nanoparticles were clearly forming clusters with a loose aspect consistent with the agglomerates measured by DLS. EDS analysis confirmed titanium as the main constituent of attached nanoparticles. No evidence of internalization was observed for TiO_2 particles. Lin *et al.* observed adhesion of TiO_2 nanoparticles to *Chlorella* sp. cells with subsequent cell wall rupture and induced plasmolysis.[53] The adhesion of TiO_2 nanoparticles could affect the transport of nutrients and

metabolites across the cell wall and membrane, which could thus inhibit algal growth.[42] In fact, TiO_2 was the more toxic nanoparticle for cyanobacteria. It is interesting to note that Fe_3O_4 nanoparticles induced cell wall undulations which would suggest cell wall damage, but no evidence of Fe_3O_4 attachment around the cell wall was found (Fig. 5f). Rogers *et al.* suggested that attached nanoparticles may cause mechanical damage to the cell membrane because of the numerous edges, corners and reactive sites present in the crystal structure of the nanoparticle.[54] TEM images of exposed cyanobacterial cells did not provide any evidence of internalization of any of the tested nanoparticles but revealed cell damage when cells were exposed to wastewater. Fig. 5g and h show extensive cytoplasmic vacuolization with thylakoid disorganization and detachment. Vacuolization and loss of the thylakoids were also observed in cells exposed to nanoparticles–wastewater binary combinations (Fig. 5i–l). Fig. 5k confirms the presence of cell wall undulations in TiO_2–wastewater exposed cells with apparent loss of cytoplasmic contents.

Electron dense granules were observed within both exposed and non-exposed cells. EDS analysis already confirmed the absence of intracellular silicon, titanium or iron in cyanobacterial cells exposed to nanoparticles. Lipid droplets have been mentioned in the literature as spherical electron-dense small granules in electron micrographs of cyanobacteria. In order to explore this possibility, confocal micrographs of *Anabaena* CPB4337 cells stained with Bodipy 505/515 dye, which is specific for neutral lipids, were obtained. Intracellular lipid droplets were identified in the cyanobacterium *Nostoc punctiforme* by staining with Bodipy 505/515.[55] Fig. S3 (ESI†) shows micrographs of chlorophyll autofluorescence and Bodipy 505/515 fluorescence of *Anabaena* CPB4337 cells non-exposed and exposed to SiO_2 and SiO_2–NH_2 nanoparticles for 24 h (as representative staining with nanoparticles). Chlorophyll autofluorescence indicated that the cells were viable. A representative filament of the non-exposed cyanobacterium is shown in Fig. S3a.† Lipid droplets were observed in control cells as densely stained inclusions showing green fluorescence. In the nanoparticle-exposed cells, Bodipy 505/515 also revealed the presence of lipid droplets (Fig. S3b and c†). Green fluorescent granules were also apparent outside the filaments which could be due to lipid droplets inside single cells detached from filaments which may not be viable, as shown by the loss of autofluorescence.

No significant cell–nanoparticle interaction was observed in the case of silica particles that could account for cytoplasmic disorganization, the main toxicity being due to the exposure to wastewater components. In the case of the more toxic TiO_2 and Fe_3O_4 nanoparticles, cell–wall interaction was the probable cause for their lower EC_{50} values (Fig. 3), but in any case cell damage could be associated with nanoparticle internalization. The non-additive effect observed (Fig. 4) could be attributed to the adsorption of wastewater pollutants on the surface of nanoparticles, which resulted in a reduced bioavailability or reverse Trojan-horse effect. Supporting this
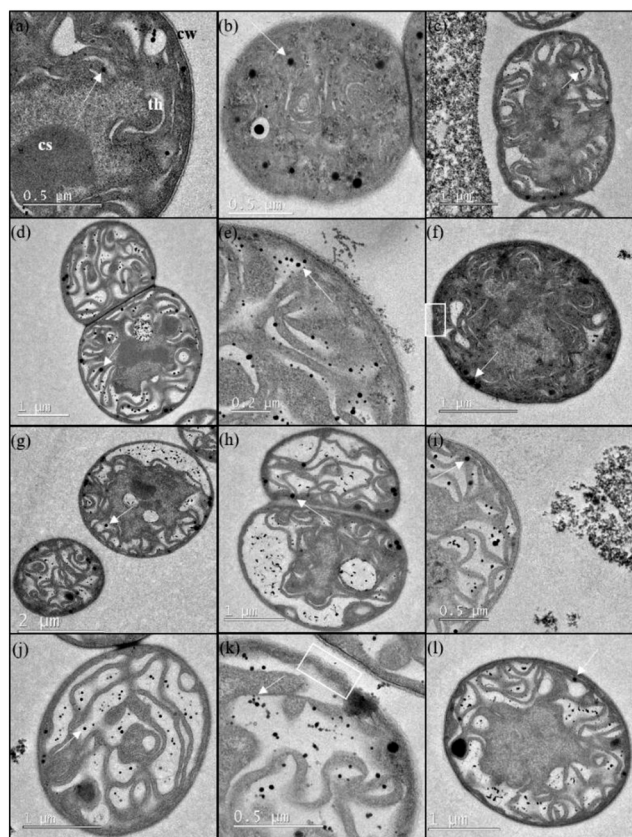

Fig. 5 High-resolution transmission electron microscopy (TEM) micrographs of *Anabaena* sp. PCC 7120 CPB4337 (a and b) non-exposed and exposed to (c) SiO_2, (d) SiO_2–NH_2, (e) TiO_2, and (f) Fe_3O_4 nanoparticles, and (g and h) wastewater for 24 h. TEM images of *Anabaena* sp. PCC 7120 CPB4337 cells in the presence of binary combinations of nanoparticles–wastewater: (i) SiO_2–wastewater, (j) SiO_2–NH_2–wastewater, (k) TiO_2–wastewater, and (l) Fe_3O_4–wastewater after 24 h of exposure. CW = cell wall, CS = carboxysome, T = thylakoid. Arrows indicate lipid droplets (see Fig. S3†). White squares indicate cell wall undulations.

hypothesis, the higher the amount of micropollutants adsorbed, the higher the antagonism observed in the lower concentration range (SiO_2 and TiO_2 nanoparticles). Our study has implications for the environmental transport, fate, and bioavailability of pollutants, which can also be altered by the release of nanooxides into the environment. Moreover, some particles such as colloidal silica and silicates, clay minerals and oxides and hydroxides of iron and aluminium are major constituents of natural colloids.[56] These natural nanoparticles can also interact with anthropogenic chemicals in a similar way to engineered nanoparticles.

Conclusions

We studied the physical (adsorption) and toxicological interaction of the micropollutants present in biologically treated wastewater with SiO_2, amino-modified SiO_2, TiO_2 (anatase) and Fe_3O_4 nanoparticles, all of them being in the 6–20 nm range. The compounds quantified comprise a group of 46 organic pollutants, mainly pharmaceuticals belonging to different therapeutic groups and some of their metabolites. The toxicity was measured as the bioluminescence inhibition of the cyanobacteria *Anabaena* sp. PCC 7120 strain CPB4337.

Nanoparticles were observed forming aggregates in the vicinity of cells or adhering to their outer surface, but without any evidence of internalization. Cell damage, consisting of cytoplasmic vacuolization and thylakoid disorganization, was attributed to wastewater components. The antagonistic effect of nanoparticles was attributed to their capacity for sequestering toxic organic compounds by adsorption on the nanoparticle surface.

The amount of micropollutants adsorbed after 24 h contact runs was 13.4 µg g^{-1}, 4.8 µg g^{-1}, 10.8 µg g^{-1} and 7.1 µg g^{-1} for SiO_2, SiO_2–NH_2, TiO_2 and Fe_3O_4, respectively. The figures account for the compounds we could unambiguously quantify at the 95% confidence level. The higher amounts adsorbed corresponded to 4AAA, 4FAA, bezafibrate, furosemide and gemfibrozil. The adsorption capacity was considerably higher for the less polar and less hydrophilic compounds. No effect associated with nanoparticle charge was observed. The difference in nanoparticle ζ-potential, which ranged from −26.5 mV (SiO_2) to +42.6 mV (Fe_3O_4), disappeared when dispersed in wastewater to yield a value essentially coincident with that of wastewater particles.

SiO_2 and SiO_2–NH_2 nanoparticles were non-toxic with EC_{50} (24 h) near 500 mg L^{-1}. TiO_2 and Fe_3O_4 nanoparticles, which were more toxic in terms of EC_{50} (14 and 33 mg L^{-1}, respectively), displayed EC_{10} values (assimilable to NOEC) higher than those of SiO_2 and SiO_2–NH_2, which were below 1 mg L^{-1}. The nanoparticle–wastewater combination displayed considerable (CI > 2) antagonism for the lower affected fractions, which corresponded to the lower concentrations assayed except for Fe_3O_4, which exhibited additive behaviour. For increased bioluminescence inhibition, a plateau was observed in the antagonism-additivity range of affected fractions.

Acknowledgements

References

1 A. Jelić, M. Gros, M. Petrović, A. Ginebreda and D. Barceló, in *Emerging and Priority Pollutants in Rivers: Bringing Science into River Management Plans*, ed. H. Guasch, A. Ginebreda and A. Geiszinger, Springer Berlin Heidelberg, Berlin, Heidelberg, 2012, pp. 1–23, DOI: 10.1007/978-3-642-25722-3_1.

2 Y. Luo, W. Guo, H. H. Ngo, L. D. Nghiem, F. I. Hai, J. Zhang, S. Liang and X. C. Wang, *Sci. Total Environ.*, 2014, **473–474**, 619–641.

3 R. Altenburger, S. Ait-Aissa, P. Antczak, T. Backhaus, D. Barcelo, T. B. Seiler, F. Brion, W. Busch, K. Chipman, M. Lopez de Alda, A. Umbuzeiro Gde, B. I. Escher, F. Falciani, M. Faust, A. Focks, K. Hilscherova, J. Hollender, H. Hollert, F. Jager, A. Jahnke, A. Kortenkamp, M. Krauss, G. F. Lemkine, J. Munthe, S. Neumann, E. L. Schymanski, M. Scrimshaw, H. Segner, J. Slobodnik, F. Smedes, S. Kughathas, I. Teodorovic, A. J. Tindall, K. E. Tollefsen, K. H. Walz, T. D. Williams, P. J. Van den Brink, J. van Gils, B. Vrana, X. Zhang and W. Brack, *Sci. Total Environ.*, 2015, **512–513**, 540–551.

4 European Commission, *Toxicity and assessment of chemical mixtures, Scientific Committee on Health and Environmental Risks (SCHER), Scientific Committee on Emerging and Newly Identified Health Risks (SCENIHR) and Scientific Committee on Consumer Safety (SCCS)*, Brussels, 2011.

5 T. Backhaus, R. Altenburger, Å. Arrhenius, H. Blanck, M. Faust, A. Finizio, P. Gramatica, M. Grote, M. Junghans, W. Meyer, M. Pavan, T. Porsbring, M. Scholze, R. Todeschini, M. Vighi, H. Walter and L. H. Grimme, *Cont. Shelf Res.*, 2003, **23**, 1757–1769.

6 M. Faust, R. Altenburger, T. Backhaus, H. Blanck, W. Boedeker, P. Gramatica, V. Hamer, M. Scholze, M. Vighi and L. H. Grimme, *Aquat. Toxicol.*, 2003, **63**, 43–63.

7 R. Altenburger, H. Walter and M. Grote, *Environ. Sci. Technol.*, 2004, **38**, 6353–6362.

8 A. Kortenkamp, T. Backhaus and M. Faust, *State of the art report on mixture toxicity. Final report to the European Commission*, 2009.

9 A. Coors and T. Frische, *Environ. Sci. Eur.*, 2011, **23**, 1–18.

10 J. R. Lead and K. J. Wilkinson, *Environ. Chem.*, 2006, **3**, 159–171.

11 I. Lynch and K. A. Dawson, *Nano Today*, 2008, **3**, 40–47.

12 A. J. Brooks, H. N. Lim and J. E. Kilduff, *Nanotechnology*, 2012, **23**, 294008.

13 Q. Jing, Z. Yi, D. Lin, L. Zhu and K. Yang, *Water Res.*, 2013, **47**, 4006–4012.

This journal is © The Royal Society of Chemistry 2017

Environ. Sci.: Nano, 2017, **4**, 1273–1282 | 1281

14 J. L. Falconer, C. F. Jones, S. Lu and D. W. Grainger, *Environ. Sci.: Nano*, 2015, **2**, 645–652.

15 J. Sanchís, M. Olmos, P. Vincent, M. Farré and D. Barceló, *Environ. Sci. Technol.*, 2016, **50**, 961–969.

16 T. C. Chou, *Pharmacol. Rev.*, 2006, **58**, 621–681.

17 R. Rosal, A. Rodríguez, J. A. Perdigón-Melón, A. L. Petre, E. García-Calvo, M. J. Gómez, A. Agüera and A. R. Fernández-Alba, *Water Res.*, 2010, **44**, 578–588.

18 M. J. Bueno, M. J. Gómez, S. Herrera, M. D. Hernando, A. Agüera and A. R. Fernández-Alba, *Environ. Pollut.*, 2012, **164**, 267–273.

19 N. Klamerth, S. Malato, A. Agüera and A. R. Fernández-Alba, *Water Res.*, 2013, **47**, 833–840.

20 I. Rodea-Palomares, F. Fernández-Piñas, C. González-García and F. Leganés, in *Handbook on Cyanobacteria: Biochemistry, Biotechnology and Applications*, ed. H. J. M. Percy and M. Gault, Nova Science Publishers, New York, 2009, pp. 283–304.

21 M. B. Allen and D. I. Arnon, *Plant Physiol.*, 1955, **30**, 366–372.

22 T. J. Norberg-King, *A linear interpolation method for sublethal toxicity: The inhibition concentration (ICp) approach*, National effluent toxicity assessment center technical report, USEPA, Duluth, MN, 1993.

23 I. Rodea-Palomares, K. Boltes, F. Fernandez-Pinas, F. Leganes, E. Garcia-Calvo, J. Santiago and R. Rosal, *Toxicol. Sci.*, 2011, **119**, 135–145.

24 I. Rodea-Palomares, A. L. Petre, K. Boltes, F. Leganes, J. A. Perdigon-Melon, R. Rosal and F. Fernandez-Pinas, *Water Res.*, 2010, **44**, 427–438.

25 T. M. Chou and N. Martin, *CompuSyn for drug combinations and for general dose-effect analysis, software and user's guide: A computer program for quantitation of synergism and antagonism in drug combinations, and the determination of IC50 and ED50 and LD50 values*, ComboSyn Inc Paramus, NJ, 2005.

26 D. Grasso, K. Subramaniam, M. Butkus, K. Strevett and J. Bergendahl, *Rev. Environ. Sci. Biotechnol.*, 2002, **1**, 17–38.

27 G. E. Brown, V. E. Henrich, W. H. Casey, D. L. Clark, C. Eggleston, A. Felmy, D. W. Goodman, M. Grätzel, G. Maciel, M. I. McCarthy, K. H. Nealson, D. A. Sverjensky, M. F. Toney and J. M. Zachara, *Chem. Rev.*, 1999, **99**, 77–174.

28 M. B. Romanello and M. M. Fidalgo de Cortalezzi, *Water Res.*, 2013, **47**, 3887–3898.

29 J. M. Pettibone, D. M. Cwiertny, M. Scherer and V. H. Grassian, *Langmuir*, 2008, **24**, 6659–6667.

30 A. Beasley, S. E. Belanger, J. L. Brill and R. R. Otter, *Environ. Toxicol. Chem.*, 2015, **34**, 2378–2384.

31 G. Carbonell, C. Fernández and J. V. Tarazona, *Bull. Environ. Contam. Toxicol.*, 2010, **85**, 72–78.

32 C. Cherchi and A. Z. Gu, *Environ. Sci. Technol.*, 2010, **44**, 8302–8307.

33 C. Wei, Y. Zhang, J. Guo, B. Han, X. Yang and J. Yuan, *J. Environ. Sci.*, 2010, **22**, 155–160.

34 K. Van Hoecke, K. A. C. De Schamphelaere, P. Van Der Meeren, S. Lucas and C. R. Janssen, *Environ. Toxicol. Chem.*, 2008, **27**, 1948–1957.

35 W. M. Lee and Y. J. An, *Chemosphere*, 2013, **91**, 536–544.

36 V. Aruoja, H. C. Dubourguier, K. Kasemets and A. Kahru, *Sci. Total Environ.*, 2009, **407**, 1461–1468.

37 K. Hund-Rinke and M. Simon, *Environ. Sci. Pollut. Res.*, 2006, **13**, 225–232.

38 V. Aruoja, S. Pokhrel, M. Sihtmae, M. Mortimer, L. Madler and A. Kahru, *Environ. Sci.: Nano*, 2015, **2**, 630–644.

39 J. B. Belden, R. J. Gilliom and M. J. Lydy, *Integr. Environ. Assess. Manage.*, 2007, **3**, 364–372.

40 J. B. Carbajo, J. A. Perdigón-Melón, A. L. Petre, R. Rosal, P. Letón and E. García-Calvo, *Water Res.*, 2015, **72**, 174–185.

41 I. Velzeboer, J. T. K. Quik, D. van de Meent and A. A. Koelmans, *Environ. Toxicol. Chem.*, 2014, **33**, 1766–1773.

42 N. B. Hartmann, F. Von der Kammer, T. Hofmann, M. Baalousha, S. Ottofuelling and A. Baun, *Toxicology*, 2010, **269**, 190–197.

43 W. W. Yang, A. J. Miao and L. Y. Yang, *PLoS One*, 2012, **7**, e32300.

44 C. Cerrillo, G. Barandika, A. Igartua, O. Areitioaurtena and G. Mendoza, *Sci. Total Environ.*, 2016, **543**(Part A), 95–104.

45 S. Gonzalo, V. Llaneza, G. Pulido-Reyes, F. Fernández-Piñas, J. C. Bonzongo, F. Leganes, R. Rosal, E. García-Calvo and I. Rodea-Palomares, *PLoS One*, 2014, **9**, e109645.

46 R. Rosal, I. Rodea-Palomares, K. Boltes, F. Fernández-Piñas, F. Leganés, S. Gonzalo and A. L. Petre, *Environ. Sci. Pollut. Res.*, 2010, **17**, 135–144.

47 K. Yang and B. Xing, *Environ. Sci. Technol.*, 2009, **43**, 1845–1851.

48 E. Lucas, S. Decker, A. Khaleel, A. Seitz, S. Fultz, A. Ponce, W. Li, C. Carnes and K. J. Klabunde, *Chem. – Eur. J.*, 2001, **7**, 2505–2510.

49 K. Yang, D. Lin and B. Xing, *Langmuir*, 2009, **25**, 3571–3576.

50 R. Rosal, I. Rodea-Palomares, K. Boltes, F. Fernández-Piñas, F. Leganés and A. L. Petre, *Chemosphere*, 2010, **81**, 288–293.

51 N. Cedergreen, *PLoS One*, 2014, **9**, e96580.

52 S. Bakshi, Z. L. He and W. G. Harris, *Crit. Rev. Environ. Sci. Technol.*, 2015, **45**, 861–904.

53 D. Lin, J. Ji, Z. Long, K. Yang and F. Wu, *Water Res.*, 2012, **46**, 4477–4487.

54 N. J. Rogers, N. M. Franklin, S. C. Apte, G. E. Batley, B. M. Angel, J. R. Lead and M. Baalousha, *Environ. Chem.*, 2010, **7**, 50–60.

55 A. Peramuna and M. L. Summers, *Arch. Microbiol.*, 2014, **196**, 881–890.

56 S. Wagner, A. Gondikas, E. Neubauer, T. Hofmann and F. von der Kammer, *Angew. Chem., Int. Ed.*, 2014, **53**, 12398–12419.

1282 | *Environ. Sci.: Nano*, 2017, **4**, 1273–1282

This journal is © The Royal Society of Chemistry 2017